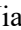






An Innovative Obstacle Avoidance Algorithm for UAV Based on Hemispherical Optimal Path

Jiandong Guo¹^a, Zhenquan Qian²^b, Mengjie Zhu³^c, Hui Liu⁴^d and Zhenguang Liu²^e

¹Key Laboratory of Unmanned Aerial Vehicle Technology of the Ministry of Industry and Information Technology, Nanjing University of Aeronautics and Astronautics, Nanjing, P. R. China

²College of Automation Engineering, Nanjing University of Aeronautics and Astronautics, Nanjing, P. R. China

³Shanghai Electro-Mechanical Engineering Institute, Shanghai, P. R. China

⁴College of Aerospace Engineering, Nanjing University of Aeronautics and Astronautics, Nanjing, P. R. China

Keywords: Obstacle Avoidance Algorithm, Path Planning, Nonlinear Guidance Law, Hemispherical Optimal Path, 3D Trajectory Tracking.


Abstract: A novel three-dimensional (3D) autonomous real-time obstacle avoidance algorithm based on hemispherical optimal path is proposed in this paper to solve the problem of obstacle avoidance during the flight for UAVs. Firstly, the irregular obstacles are modelled by one or more hemispheres, which are used to cover the whole or key parts of the obstacles. Then, the avoidance strategy is obtained and the optimal arc avoidance trajectory is calculated according to the geometric relationship between the obstacle model and UAV, and the obstacle avoidance problem is transformed into the avoidance trajectory tracking problem. Finally, according to the fixed distance limit of the nonlinear guidance parameters, the variable gain virtual reference point is designed, the stability condition of trajectory tracking is analyzed, and combined with altitude guidance law to develop the 3D trajectory tracking control and autonomous real-time obstacle avoidance. The nonlinear numerical simulation of a type of UAV shows that the presented obstacle avoidance algorithm can avoid obstacles effectively with high accuracy for 3D trajectory tracking, which can be applied to UAV's obstacle avoidance missions.


1 INTRODUCTION


Unmanned aerial vehicles (UAV) have been widely used in civil and military fields due to their advantages of flexibility, portability, mobility, and concealment (Mairaj et al., 2019; Hildmann and Kovacs, 2019). However, the flight environment will become more and more complex with the continuous development of UAV, the autonomous obstacle avoidance technology of UAV will gradually become one of the key technologies (Lacono and Sgorbissa, 2018; Wan et al., 2019).


The obstacle avoidance methods for UAV can be mainly divided into the following two categories: (1)


The first method is based on path planning, the main idea of this method is to convert the obstacle avoidance problem to path planning problem. With the development of research in this field, many path planning approaches have been proposed, such as genetic algorithm (GA) (Elhoseny et al., 2018; Kwasniewski and Gosiewski, 2018), artificial potential field (APF) (Tang et al., 2019; Zhang et al., 2018), A* algorithm (Gochev et al., 2017), RRT (Zu et al., 2018), etc., these algorithms are compared in terms of time of computation and optimality of solution in different scenarios and obstacle layouts (Radmanesh et al., 2018; Zammit and Erik-Jan, 2018), which find that the GA shows less

^a <https://orcid.org/0000-0002-4733-2550>

^b <https://orcid.org/0000-0003-0361-8546>

^c <https://orcid.org/0000-0003-2643-490X>

^d <https://orcid.org/0000-0003-0253-9651>

^e <https://orcid.org/0000-0002-8121-2990>

sensitivity to time with respect to the increase number of cells; the APF shows a reasonable time of solution, but poor ability to overcome the local minima and provides non-optimal results; the A* algorithm shows the ability to solve the scenarios optimally by spending considerably higher computational time, the RRT algorithm shows faster converges, but is often not optimal. In general, there is a trade-off between the optimality and computational time requirements in path planning algorithms (Agarwal and Bharti, 2018). (2)The second method based on geometrical relationships, the main idea of this method is to calculate the guidance law of avoidance manoeuvre according to the relative distance, speed, acceleration, angle etc., between UAV and obstacles. The UAV avoids obstacle (Sasongko et al., 2017) by tracking obstacle avoidance waypoints, which is calculated through the obstacle model and UAV's speed vector. The fuzzy rules are established based on the forward speed of UAV and the distance between UAV and obstacles, then the heading command of the obstacle avoidance behavior is obtained through fuzzy logic control to realize the obstacle avoidance (Zhang et al., 2018), due to the complexity of this method, it can only deal with two-dimensional UAV obstacle avoidance problem. The UAV avoids the obstacle by flying along the safe flight boundary consisted of a number of feature points (Ai-kaff et al., 2017), which are obtained by detecting the position relationship between UAV and obstacles in real time. In brief, the obstacle avoidance method based on geometric relationship has a good real-time performance, but it usually needs to model the obstacles, which is difficult to apply in complex flight conditions (Ha et al., 2019).

This paper proposes an innovative 3D real-time obstacle avoidance algorithm which is implemented on UAV autonomous guidance system, to provide a capability of adjusting its flight direction when there is a possibility of collision on the target trajectory. This method uses the hemispheres to model obstacle according to the known or detected information by sensors, the entire or critical part of the obstacle can be covered by one or more hemispheres. Then the obstacle avoidance strategy is designed, with the shortest arc avoidance trajectory is calculated according to the geometric relationship between the obstacle model and the UAV, so that the obstacle avoidance problem is transformed into the avoidance trajectory tracking problem. Finally, the guidance laws are combined with the lateral guidance (Park et al., 2004) and altitude guidance, which is utilized to realize autonomous obstacle avoidance and trajectory tracking for the UAV.

2 MODELLING OF OBSTACLE

When UAV is under the flight missions, there are many obstacles in the predefined flight path, such as buildings, mountains, trees, etc., which affect the completion of flight missions and the safety of the aircraft directly. Therefore, pre-processing of the obstacle is the first step for designing obstacle avoidance algorithm.

2.1 Obstacle Hemisphere Model

The most obstacles are often irregular in real flight scene, making difficult to model, and the obstacle information detected by onboard sensors is often not enough. In addition, too much attention on the details of the obstacles will greatly increase the design difficulty and calculation amount of calculation, reduce the obstacle avoidance effect. Hence, a suitable obstacle model is critical to the design of obstacle avoidance algorithms.

In this paper, the standard convex hemisphere is selected to model the obstacle, according to the obstacle information detected by on-board detector, the whole or key part of the obstacle is covered with a suitable hemisphere. The mathematical expression of the hemisphere is given as:

$$\Gamma = \left(\frac{x-x_0}{R}\right)^2 + \left(\frac{y-y_0}{R}\right)^2 + \left(\frac{z-z_0}{R}\right)^2, \quad z \geq z_0 \quad (1)$$

Where (x_0, y_0, z_0) and R are represent the coordinate of the centre point and radius of the obstacle. $\Gamma < 1$, $\Gamma = 1$ and $\Gamma > 1$ represent internal, tangency and external of the obstacle, respectively.

Therefore, the obstacles can be described by only two parameters, namely centre and radius, which simplifies the design of obstacle avoidance algorithm. In addition, this modelling approach can also be extended to describe a complex obstacle with multiple hemispheres.

2.2 Hemisphere Determination

When UAV detects an obstacle under the predefined flight path, a series of sampling points are obtained by on-board sense sensor, such as infrared camera, Lidar, and so on. Therefore, a regular sphere can be fitted according to those sampling points by the Least Square method. Let,

$$Y = x^T x + y^T y + z^T z \quad (2)$$

Where x, y, z is the matrix of sampling points boundary coordinates, define,

$$K = (H^T H)^{-1} H^T Y \quad (3)$$

Where,

$$H = [x, y, z, 1_{n \times 1}] \quad (4)$$

Hence, the centre coordinate $[o_x, o_y, o_z]^T$ and radius r of the sphere are obtained by the sampling points as:

$$\begin{bmatrix} o_x \\ o_y \\ o_z \end{bmatrix} = \frac{1}{2} \begin{bmatrix} K(1) \\ K(2) \\ K(3) \end{bmatrix} \quad (5)$$

$$r = \sqrt{o_x^2 + o_y^2 + o_z^2 + K(4)} \quad (6)$$

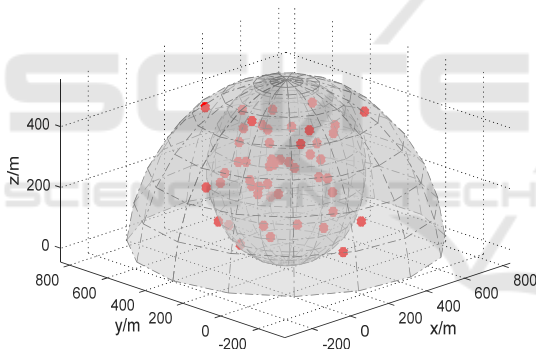


Figure 1: Hemisphere determination from sampling points.

The sphere obtained by this fitting method can't cover all sampling points, and the sampling points can't represent obstacle completely yet, which is limited by sensor capabilities. A hemisphere model slightly larger than the sphere can be determined, the centre coordinate and radius of hemisphere is the bottom and twice radius of the sphere, respectively. The equation of the hemisphere is:

$$(x-o_x)^2 + (y-o_y)^2 + (z-o_z-r)^2 = (2r)^2, z \geq o_z + r \quad (7)$$

3 OBSTACLE AVOIDANCE ALGORITHM BASED ON OPTIMAL PATH

After pre-processing of obstacles in flight scenes, the hemisphere obstacle model is obtained. In order to make the UAV track the predefined waypoints path without obstacle offending, a novel obstacle avoidance algorithm based on hemispherical optimal path is designed, and the avoidance rules are determined.

3.1 Obstacle Detection and Avoidance Determination

Design a suitable virtual "line-of-sight" L_{det} according to the aircraft flight performance and obstacle size, which is a constant and consistent with aircraft flight direction, it is important to determine if the aircraft intersects the obstacle. As shown in the left of Figure 2, the line of sight is the shortest one when UAV avoids obstacles with the minimum turning radius, then the minimum detection line $L_{det,min}$ is obtained by Pythagorean theorem as,

$$L_{det,min} = \sqrt{R_{obs}^2 + 2R_{min}^2} - R_{obs} \quad (8)$$

Where R_{obs} is the radius of the corresponding hemisphere circle at the local altitude for the aircraft, R_{min} represents the minimum turn radius of the aircraft and is given,

$$R_{min} = V_n^2 / g \tan(\phi_{max}) \quad (9)$$

Where V_n and ϕ_{max} are the ground speed and the maximum roll angle of the UAV, respectively.

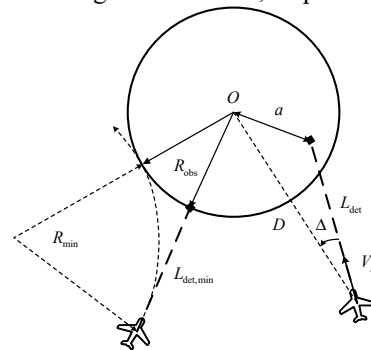


Figure 2: Obstacle detection geometry logic.

In order to obtain the final value of L_{det} , additional compensation factors must be considered for the roll angle delay time t_{roll} , which is from the initial angle to ϕ_{max} . Then the delayed distance can be obtained with V_n multiply by t_{roll} , which is added to $L_{det,min}$, then L_{det} is given as following,

$$L_{det} = L_{det,min} + V_n t_{roll} \quad (10)$$

Eq. (11) satisfies as,

$$D \leq L_{det} + R_{obs} \quad (11)$$

Where, D is the distance between UAV and the centre of circle, which means that the UAV starts to detect the obstacles. As shown in Figure 2, if $a = R_{obs}$, the end of the detection line is on the edge of the obstacle, if $a \leq R_{obs}$, the detection line touches the obstacle, the aircraft needs to avoid flight action to be away from the obstacle, where a is the segment obtained by the centre of circle and the end of the detection line.

3.2 Optimal Avoidance Path

As depicted in Figure 3, WP_1, WP_2 are two waypoints on target path, the coordinates in the East-North-Up (ENU) frame are $(wp_{1,E}, wp_{1,N}, wp_{1,U})$ and $(wp_{2,E}, wp_{2,N}, wp_{2,U})$, respectively. The spatial straight line equation of the two waypoints is:

$$\frac{x - wp_{1,E}}{wp_{2,E} - wp_{1,E}} = \frac{y - wp_{1,N}}{wp_{2,N} - wp_{1,N}} = \frac{z - wp_{1,U}}{wp_{2,U} - wp_{1,U}} \quad (12)$$

Suppose the centre coordinate and radius of the hemisphere are (c_E, c_N, c_U) and R . According to Eq. (7) and Eq. (12), the intersection points M and N of the straight line and the hemisphere model can be calculated. Hence, the shortest distance between the two points on the spherical surface is the inferior arc through the maximum circle, which passes through the intersection points M and N , and coincides with the centre of the hemisphere. The parametric equation for the circle about points M, N and centre C is given as:

$$\begin{cases} x = c_E + m_E R \cos \rho + n_E R \sin \rho \\ y = c_N + m_N R \cos \rho + n_N R \sin \rho \\ z = c_U + m_U R \cos \rho + n_U R \sin \rho \end{cases} \quad (13)$$

Where, the unit vector $\vec{m} = (m_E, m_N, m_U)$ and $\vec{n} = (n_E, n_N, n_U)$ are perpendicular to each other and perpendicular to the circular normal vector, and parameter $\rho \in [0, 2\pi]$.

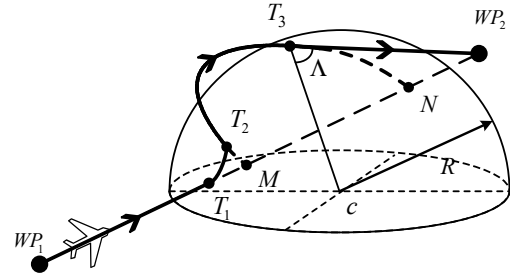


Figure 3: Obstacle avoidance problem & optimal avoidance path determination.

When the UAV detects obstacle threat at the point T_1 , the inferior arc \widehat{MN} is calculated in real time, which is the shortest avoidance path. Then the UAV completes the obstacle avoidance by tracking the optimal avoidance path, then the obstacle avoidance problem is transformed into the path following problem. To ensure that the UAV can avoid obstacles safely, set the hemisphere obstacle radius is $(R + L_{safe})$, where L_{safe} is safe flight distance.

3.3 Avoidance Success Criteria

During the obstacle avoidance fight, the UAV detects and judges continuously whether the desired waypoint is reachable. If the desired waypoint is not in the obstacle, it means that the desired waypoint is reachable, otherwise it switches to the next waypoint of the desired waypoint.

We can compute the angle Λ to determine whether avoidance is over, which is the angle between the segment made by the UAV's and the next valid waypoint, and the segment made by the UAV's and the centre of the obstacles. As soon as $\Lambda \geq \pi / 2$ at point T_3 , means that there is a line of sight to the next valid waypoint. Then the UAV ends the avoidance flight and flies to the valid waypoint in straight trajectory.

The avoidance procedure, connecting with the waypoint guidance procedure, is described in Figure4.

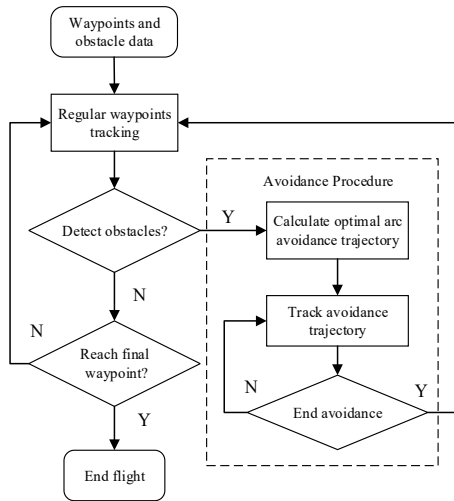


Figure 4: Waypoints path tracking and obstacle avoidance procedure.

4 GUIDANCE SYSTEM

The guidance system and obstacle avoidance algorithm are mainly responsible for generating a set of maneuver commands to drive the drone as close as possible to the predefined and avoidance path. Therefore, the performance of guidance system is very important to the aircraft.

4.1 Lateral guidance law

The nonlinear guidance law was first implemented on UAV by Park (Park et al., 2004). The basic principle of the guidance law is to select a reference point P on the target trajectory, with a fixed distance L_1 away from the UAV, which is utilized to produce a lateral acceleration instruction a_L according to the position about the reference point and the current the UAV, as described in Figure 5. The desired lateral acceleration is:

$$a_L = (2V_n^2 / L_1) \sin \eta \tag{14}$$

Where η is the angle between the UAV ground speed vector V_n and the L_1 line segment vector, can expression as:

$$\eta = \arcsin \frac{V_n \times L_1}{|V_n| |L_1|} \tag{15}$$

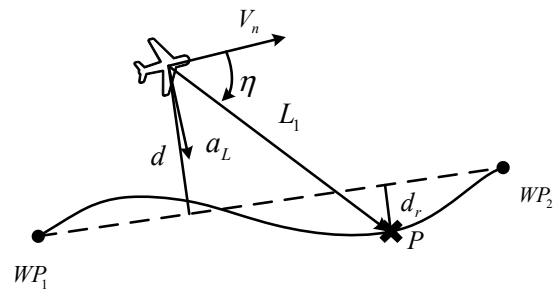


Figure 5: Lateral guidance law geometry logic.

Literature (Park et al., 2007) shows the following transfer function between the lateral deviation of the UAV and the reference point from the nominal straight line, which describes the response of the system as:

$$\frac{d(s)}{d_r(s)} = \frac{\omega_n^2}{s^2 + 2\xi\omega_n + \omega_n^2} \tag{16}$$

Where $\xi = 0.707$, $\omega_n = \sqrt{2}V_n / L_1$. Note that the pole location depends on the values L_1 and V_n , since L_1 is a fixed value, the value of V_n directly affects the stability of the system and the gain of the controller. In order to ensure that the amplitude-frequency characteristics of the system do not change under certain disturbances, the value of V_n is used to adjust the value of L_1 dynamically, which improves the tracking accuracy.

$$L_1 = TV_n, \quad \frac{\sqrt{2}}{\omega_n} = \frac{L_1}{V_n} = T \tag{17}$$

In order to explore the effects of constant T affects the system stability, the roll dynamics is modelled as a first order inertial, the block diagram is shown in Figure 6.

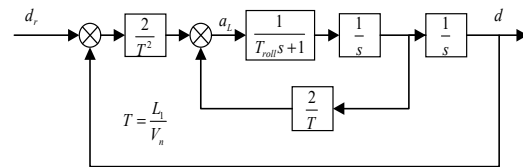


Figure 6: Block diagram of guidance law with roll dynamics.

In Figure 6, the definition T_{roll} is the first order time constant of the roll angle response to roll commands. A root locus can be constructed for

various values of T using the characteristic equation for the system:

$$\frac{T^2 T_{roll}}{2} s^3 + \frac{T^2}{2} s^2 + Ts + 1 = 0 \quad (18)$$

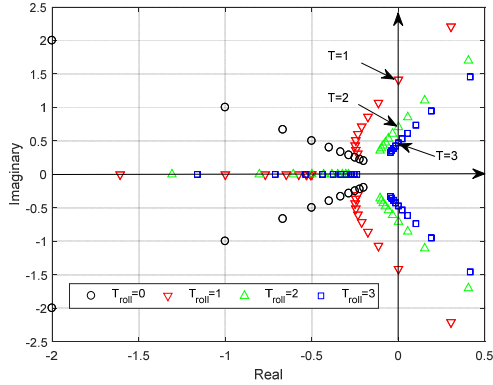


Figure 7: Root locus of characteristic equation.

The root locus of Figure 7 is constructed for $T = \{0.5:0.5:5\}$ and $T_{roll} = \{0,1,2,3\}$, it is clearly shows that when $T_{roll} = 0$, there is no inertia element in the roll angle response, all roots are in the left half plane, hence, the system is stable and is not affected by the constant T ; when $T_{roll} \neq 0$, if $T < T_{roll}$, system is unstable; if $T = T_{roll}$, system is marginally stable; if $T > T_{roll}$, system is stable. Therefore it must be ensured that the constant T is always bigger than the first time order constant T_{roll} .

Given the results of the root locus analysis, it is shown that T can be determined at least 3 to 4 times more than the first time order constant T_{roll} to ensure satisfactory transient response. Substituting Eq.17 into Eq.14 provides the new a_L is:

$$a_L = (2V_n/T) \sin \eta \quad (19)$$

The desired roll angle which can be obtained according to the kinematics equation of the UAV is,

$$\phi_c = \arctan(a_L/g) \quad (20)$$

In order to solve the problem for non-smoothing at the waypoint switching, the arc waypoints switching strategy is designed to deal with the overshoot problem during the switching waypoints, also reduces the cross-track error effectively.

As shows in Figure 8, the target path consists of three waypoints WP_1, WP_2 and WP_3 . The turn angle β is given as:

$$\beta = \arccos((\vec{q}_1 \cdot \vec{q}_2) / (|\vec{q}_1| |\vec{q}_2|)) \quad (21)$$

Where \vec{q}_1, \vec{q}_2 are the position vectors of WP_2 to WP_1 and WP_2 to WP_3 , respectively.

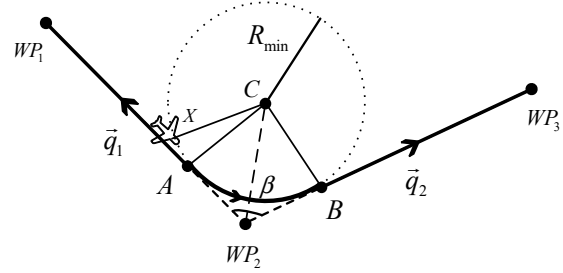


Figure 8: Waypoint switching geometry logic.

- Turn centre: The turn centre is determined at the distance of $R_{min}/\sin(\beta/2)$ from WP_2 on the line bisecting the turn angle β .
- Turn start criterion: The turn start point is at a distance of $R_{min}/\tan(\beta/2)$ from the WP_2 on the line linking WP_1 to WP_2 . Turning is starting when the cross-product $\vec{CX} \times \vec{CA}$ changes sign.
- Turn stop criterion: The turn stop point is at the distance of $R_{min}/\tan(\beta/2)$ from the WP_2 on the line joining the WP_2 and WP_3 . Turning is ended when the cross-product $\vec{CX} \times \vec{CB}$ changes sign.

4.2 Altitude Guidance Law

In this paper, taking the 3D path following problem of the aircraft as horizontal and altitude path tracking, the horizontal trajectory tracking control signal is the roll angle obtained by lateral guidance law, and the altitude tracking control signal is h_c can be obtained as follows:

$$h_c = h_1 + d_1 \cos \lambda \tan \gamma \quad (22)$$

Where, γ is the flight path angle, d_1 is the distance from the UAV to the WP_1 under horizontal projection. λ is the angle between the segment made by the UAV's centre and WP_1 , and the target path under horizontal projection, as shown in Figure 9.

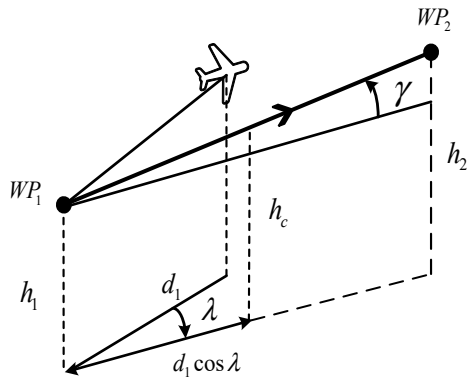


Figure 9: Altitude guidance law geometry logic.

5 SIMULATION AND ANALYSIS

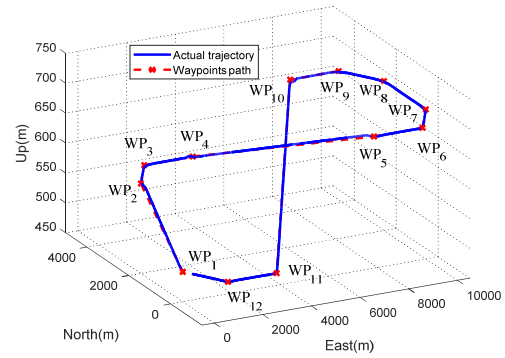
In order to verify the effectiveness of the proposed autonomous obstacle algorithm and guidance strategy, the numerical simulations are done by a 6-DOF nonlinear flight dynamics model for a fixed-wing UAV. The overall aerodynamic parameters of the aircraft model are described in (Yang et al., 2013). The restrictions of the UAV are maximum roll angle $\phi_{\max} = 30^\circ$, maximum pitch angle $\theta_{\max} = 20^\circ$. Set the initial position of the UAV is $(0, 0, 500)m$ in ENU coordinate, the cruising speed $V = 50m/s$, and the initial speed direction is the true north. Unless otherwise specified, the predefined states of the UAV in all simulation tests are the same.

5.1 Path Following Simulation

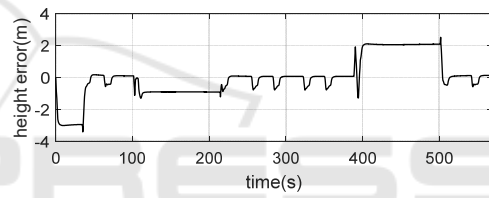
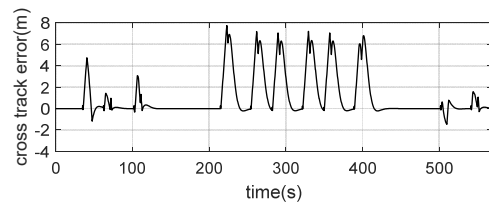
For the path following simulation, the target route consists of a set of waypoints, and the waypoints coordinate data in ENU coordinate is listed in Table 1.

Table 1: Waypoints coordinate of path following.

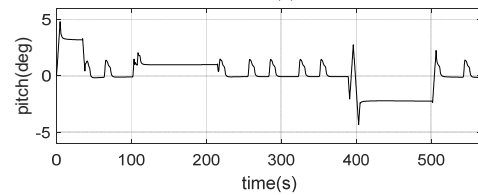
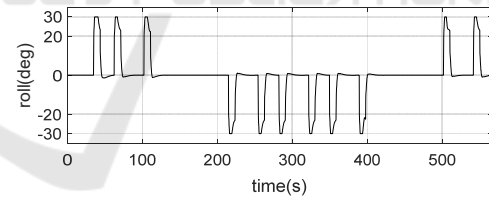
Waypoints	Coordinate (km)	Waypoint s	Coordinate (km)
WP1	(0,0,0.5)	WP7	(10,0,0.7)
WP2	(2,0,0.6)	WP8	(10,2,0.7)
WP3	(1,3,0.6)	WP9	(9,3,0.7)
WP4	(3,3,0.6)	WP10	(7,3,0.7)
WP5	(7,-1,0.7)	WP11	(3,-1,0.5)
WP6	(9,-1,0.7)	WP12	(1,-1,0.5)



(a)



(b)



(c)

Figure 10: Flight simulation of 3D path following control. (a) 3D view (b) Euler angle (c) Tracking error.

It can be seen from Figure 10 (a), the UAV tracks the predefined waypoints path accurately, and transform waypoints with circular arc path. Figure 10 (c) shows the tracking error during path following, when the UAV is tracking the path in straight

segments, the cross track error is almost 0, when the UAV begins switching waypoints, the error is within $\pm 6m$, and $\pm 2.5m$ in tracking circular arc path. Additionally, the height error is within $\pm 4m$, in a word, the UAV tracks the whole waypoints path with small error. Figure 10 (d) shows the Euler angle response of the UAV, in straight segments, roll angle response is almost 0, while the UAV tracks the circular arc path with maximum roll angle in waypoints switching segment. Similarly, the UAV has a certain pitch angle response during the climb or descent, and no response in stable altitude, but due to the effect of coordinated turn of the UAV in waypoints switching segments, a certain pitch angle response will be generated.

5.2 Obstacle Avoidance Simulation

As mentioned in the Sect.2, obstacles can be modelled by one or more hemispheres. For simple obstacles, one hemisphere is utilized to cover the whole or the key parts of the obstacle. For complex obstacles, the avoidance model can be developed by multiple cross hemispheres. Before the simulation, the obstacle hemisphere model has been fitted according to obstacle data detected by on-board detection system.

5.2.1 Simple Obstacle Avoidance

For the simple obstacle avoidance simulation, the UAV faces an obstacle threat during tracking waypoints path, which intersects with target path. The pre-defined waypoints coordinate and obstacle data are listed in Table 2. Set the safe flight distance $L_{safe} = 100m$.

Table 2: Waypoints and simple obstacle data.

Waypoints	Coordinate(km)	Obstacle	Date(km)
WP1	(0,0,0.5)	Centre	(0.5,2,0)
WP2	(0,4,0.5)	Radius	0.9
WP3	(1.2,4,0.5)		
WP4	(1,0.7,0.5)		

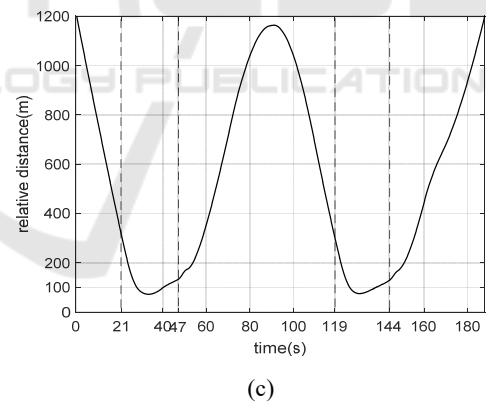
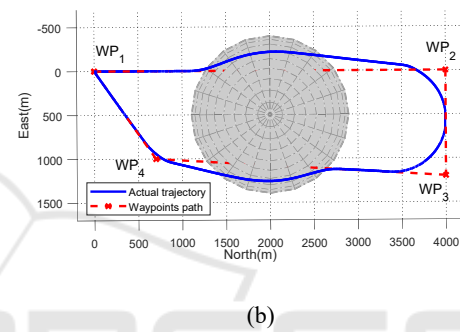
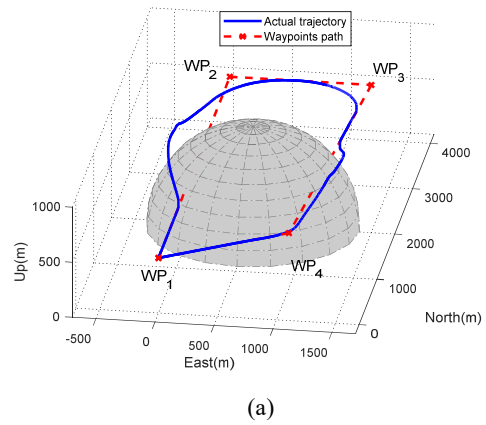


Figure 11: Flight simulation of simple obstacle avoidance. (a) 3D view (b) 2D view (c) Relative distance.

As shown in Figure 11, at first, UAV tracks the predefined waypoints path, and the obstacle is detected for the first time by on-board detection system at 21s. Then a shortest circular arc path is generated according to the geometric relationship between waypoints path and obstacle model, the guidance strategy performing maneuver operation lets the UAV track the optimal avoidance path, and complete avoidance flight at 47s, after that, UAV flies

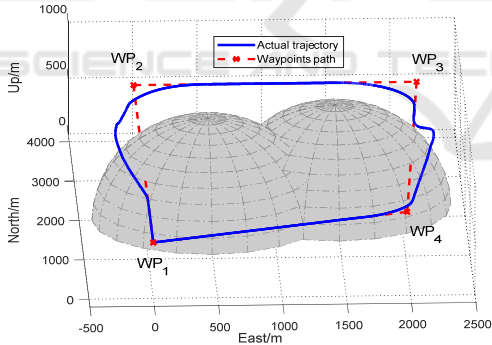
in straight line to the next reachable waypoint and continues to fly along the target path. Between 119~144s, UAV detects the obstacle threat and generates optimal circular arc path again, and performs the second avoidance action to realize obstacle avoidance. Figure 11 (c) shows the relative distance between the aircraft and the surface of obstacle during the whole flight, we can see that UAV has always been the outside of the obstacle and about 100m away from the obstacle. Therefore, it can be confirmed that the obstacle avoidance algorithm designed in this paper can effectively avoid simple obstacle.

5.2.2 Complex obstacle avoidance

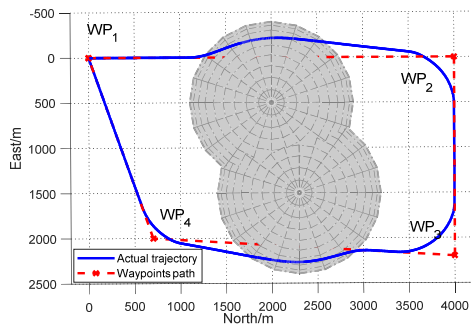
In order to verify the algorithm is also effective for complex obstacle, there is a complex obstacle consisted of two hemisphere models between waypoints path. The waypoints coordinate and obstacle date are listed in Table 3.

Table 3: Waypoints and complex obstacles date.

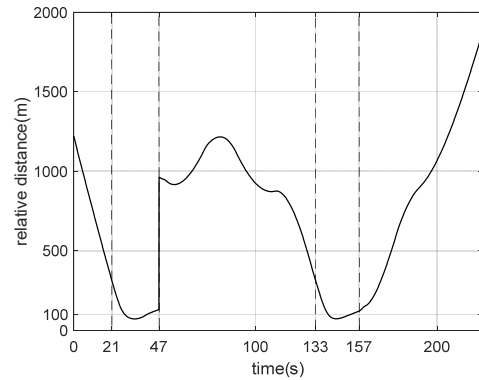
Waypoints	Coordinate(km)	Obstacles	Date(km)
WP1	(0,0,0.5)	Centre1	(0.5,2,0)
WP2	(0,4,0.5)	Centre2	(1.5,2.3,0)
WP3	(2.2,4,0.5)	Radius	0.9
WP4	(2,0.7,0.5)		



(a)



(b)



(c)

Figure 12: Flight simulation of the complex obstacle avoidance. (a) 3D view (b) 2D view (c) relative distance.

It can be seen from Figure 12, the UAV detects two obstacle threats and avoids obstacles successfully during the flight simulation. The UAV detects and avoids obstacle I&II between 21~47s and 133~157s, respectively, and the UAV has always been the outside of the obstacle and about 100m away from the obstacle. The avoidance algorithm can avoid complex obstacle effectively.

6 CONCLUSIONS

In this paper, a 3D autonomous real-time obstacle avoidance algorithm based on hemispherical path optimal is proposed. The main contributions of this research are as follows.

- 1) Mathematical model of obstacles with one or more hemispheres greatly simplifies obstacle avoidance algorithm design.
- 2) Transform obstacle avoidance problems into trajectory tracking problems to realize the optimal obstacle avoidance trajectory.
- 3) Design the variable gain virtual reference point nonlinear guidance law and arc waypoint switching strategy, which effectively improves the trajectory tracking accuracy.
- 4) The 3D trajectory tracking and obstacle avoidance simulations verify the effectiveness of the autonomous obstacle avoidance algorithm, with considering the limitations and kinematics of the UAV itself, which reveals to a good applicability in practical engineering.

Beyond that, to accomplish the fundamental purpose of the UAV trajectory planning and collision avoidance, (1) the known obstacle model is pre-set in flight control computer, the drone follows the arc path

according to the designed hemispherical convex in flight experiment; (2) the laser radar is installed on a drone to collect the obstacle feature points and fit the model in real time, using to evaluate the accuracy of the obstacle modelling.

ACKNOWLEDGMENTS

This research was made possible by Fundamental Research Funds for the Central Universities Grant No. 56XAC22030.

REFERENCES

- Agarwal, D., and Bharti, P. S. (2018). A review on comparative analysis of path planning and collision avoidance algorithms. *International Scholarly and Scientific Research & Innovation*, 12(6):608-624.
- Ai-kaff, A., Garcia, F., Martin, D., Escalera A. D. L., and Armingol, J. M. (2017). Obstacle detection and avoidance system based on monocular camera and size expansion algorithm for UAVs. *Sensors*, 17(5):1061-1082.
- Elhoseny, M., Tharwat, A., and Hassanien, A. E. (2018). Bezier curve based path planning in a dynamic field using modified genetic algorithm. *Journal of Computational Science*, 25:339-350.
- Gochev, M. I., Nadzinski, M. G., and Stankovski, D. M. (2017). Path planning and collision avoidance regime for a multi-agent system in industrial robotics. *International Scientific Journal "Machines Technologies Materials"*, 11:519-522.
- Ha, L. N. N. T., Bui, D. H. P., and Hong, S. K. (2019). Nonlinear control for autonomous trajectory tracking while considering collision avoidance of UAVs based on geometric relations. *Energies*, 12:1551-1570.
- Hildmann, H., and Kovacs, E. (2019). Review: Using unmanned aerial vehicles (UAVs) as mobile sensing platforms (MSPs) for disaster response, civil security and public safety. *Drones*, 59(3):1-26.
- Kwasniewski, K. K., and Gosiewski, Z. (2018). Genetic algorithm for mobile robot route planning with obstacle avoidance. *Acta Mechanica et Automatica*, 12(2):151-159.
- Lacono, M., and Sgorbissa, A. (2018). Path following and obstacle avoidance for an autonomous UAV using a depth camera. *Robotics and Autonomous Systems*, 106:38-46.
- Mairaj, A., Baba, A. I., and Javaid, A. Y. (2019). Application specific drone simulators: Recent advances and challenges. *Simulation Modelling Practice and Theory*, 94:100-117.
- Park, S., Deyst, J., and How, J. P. (2004). A new nonlinear guidance logic for trajectory tracking. In *2004 AIAA Guidance, Navigation, and Control Conference and Exhibit (GNCCE)*, pages:1-16. AIAA.
- Park, S., Deyst, J., and How, J. P. (2007). Performance and Lyapunov stability of a nonlinear path following guidance method. *Journal of Guidance, Control, and Dynamics*, 30(6):1718-1728.
- Radmanesh, M., Kumar, M., Guentert, P. H., and Sarim, M. (2018). Overview of path-planning and obstacle avoidance algorithms for UAVs: a comparative study. *Unmanned Systems*, 6(2): 95-118.
- Sasongko, R. A., Rawikara, S. S., and Tampubolon, H. J. (2017). UAV obstacle avoidance algorithm based on ellipsoid geometry. *Journal of Intelligent & Robotic Systems*, 88(2-4):567-581.
- Tang, J., Sun J., Lu, C., and Lao, S. (2019). Optimized artificial potential field algorithm to multi-unmanned aerial vehicle coordinated trajectory planning and collision avoidance in three-dimensional environment. In *Proceedings of the Institution of Mechanical Engineers, Part G: Journal of Aerospace Engineering*, 233(16): 6032-4043.
- Wan, Y., Tang, J., and Lao, S. (2019). Research on the collision avoidance algorithm for fix-wing UAVs based on maneuver coordination and planned trajectories prediction. *Applied Sciences*, 798(9):1-20.
- Yang, X., Mejias, L., and Bruggemann, T. S. (2013). A 3D collision avoidance strategy for UAVs in a non-cooperative environment. *Journal of Intelligent & Robotic Systems*, 70:315-327.
- Zammit, C., and Erik-Jan, V. K. (2018). Comparison between A* and RRT algorithms for UAV path planning. In *2018 AIAA Guidance, Navigation, and Control Conference (GNCC)*, pages 1-23. AIAA.
- Zhang, J., Liu, B., Meng, Z., and Zhou Y. (2018). Integrated real time obstacle avoidance algorithm based on fuzzy logic and L1 control algorithm for unmanned helicopter. In *2018 Chinese Control and Decision Conference (CCDC)*, pages 1865-1870.
- Zhang, J., Yan, J., and Zhang, P. (2018). Fixed-Wing UAV formation control design with collision avoidance based on an improved artificial potential field. *IEEE ACCESS*, 6:78342-78351.
- Zu, W., Fan, G., Gao, Y., Ma, Y., Zhang, H., and Zeng, H. (2018). Multi-UAVs cooperative path planning method based on improved RRT algorithm. In *2018 IEEE International Conference on Mechatronics and Automation (ICMA)*, pages 1563-1567. IEEE.